

Fusion of Segmented Image Using Level Set Method and Chair-Varshney Fusion Rule

Sakulrat Thammathiwat

Department of Electrical Engineering
Kasetsart University
Bangkok, Thailand
Email: sakulrat.t@ku.th

Teerasit Kasetkasem

Department of Electrical Engineering
Kasetsart University
Bangkok, Thailand
Email: fengtsk@ku.ac.th

Abstract— In this paper, we addressed the problem of combining multiple segmented images to a single segmented image. The idea is to change the fusion problem into the boundary detection problem where boundaries from each input segmented images are extracted, and then fused based on the Chair-Varshney fusion rule. Next, the level set method is employed to join and complete the fused boundaries. The evolution of level set function is conceptually stopped when the active contours moves toward the fused result.

Keywords: *CVR, edge fusion, edge indicator, image segmentation, level set method.*

I. INTRODUCTION

THE IMAGE classification and the image segmentation have closely related objectives. Classification algorithms aim to divide the image in classes by based on some prior pre-defined classes. In contrast, the goal of segmentation algorithms is to divide an image into homogenous regions based on some similarity measure. Hence, the number of segmentations of the same input images may not be the same when different segmentation algorithms are employed, and even when the number of segmentations are the same, the segmented image may appear differently. As a result, the decision fusion approaches works with classified data may not be able to apply to fuse segmented images.

The image segmentation problem can be considered as the boundary extraction problem where the goal is to insert boundaries between two or more homogeneous but different regions. Hence, when an image is segmented, boundaries will be inserted into an image. If all segmentation algorithms perform the same these boundaries will be occurred at the same location in the image and the number of boundary will be exactly the same. However, since different segmentation algorithms have different objectives, these boundaries may not be perfectly aligned. As a result, we proposed the use of a cost function to evaluate whether a boundary should actually be presented on an image or not. For example, if at the location (x,y) , all 10 segmented images from different sources agree that there should be a boundary on this point, it is likely that a point (x,y) should be a boundary point. However, if only one segmented image indicates a point (x,y) as a boundary point

when other 9 images indicate no, it is unlikely that this point is a boundary point. To achieve this goal, the Chair-Varshney fusion rule [11] is employed where the boundaries from input segmented images are fused in accordance with the accuracy of each input images in identifying boundaries. The main reason to unequal weights because different segmentation algorithms [14] segment an image differently. The Chair-Varshney rule based on a log likelihood ratio test (LRT) is the optimum fusion rule in term of probability of error.

Next, since the boundary of the same object from different segmented images may locate at exactly the same location due to many factors, including image resolutions, noise in an image, and the failure of segmentation algorithm, the resulting segmented image under the Chair-Varshney alone may have broken boundaries, incomplete edges, or multiple edges at the same location. The remedy to this problem is to employ the level set function [15] to represent the boundaries of the resulting segmented image. The level set method, extensively used as numerical method for tracking dynamic interfaces and shapes, is the mentioned formulation. This method was introduced by Osher and Sethian [1], and it was increasing notable in image segmentation in recent years. Moreover, this approach was presented independently by Caselles et al. [2] and Malladi et al. [3] in the background of traditional active contour model (ACM), which was proposed by Kass et al. [4]. In the level set method, contours or surfaces are represented as the zero level set of a higher dimensional function, usually called a *level set function*. Since this function is required to be smooth, the broken edges and incomplete contour will be removed.

Existing level set methods for image segmentation can be categorized into two major classes: region-based models [7], [13] and edge-based models [3], [5], [6]. These two types of models both have their advantages and disadvantages, and the choice of them in applications depends on different characteristics of images. Region-based models aim to identify each region of interest by using a certain region descriptor to guide the motion of the active contour. Edge-based models use edge information for image segmentation. Generally, it uses an *edge indicator function* in order to serve the purpose of stopping the evolution of the interface when it arrives at the object boundaries.

This paper is organized as follows. In Section II, we first proposed the edge indicator function with the Chair-Varshney fusion rule. In Section III, we apply the proposed general formulation to an edge-base model for image segmentation, and describe its implementations. Experimental results are shown in Section IV. Finally, some concluding remarks are provided in Section V.

II. PROPOSED EDGE INDICATOR FUNCTION

Let Ω be an open bounded subset of \Re^2 , with its boundary $\partial\Omega$, and let $\phi : \Omega \rightarrow \Re$ be a level set function defined on a domain Ω . Next, we define a total energy function for a given level set function as

$$\mathcal{E}(\phi) = \mathcal{E}_{ext}(\phi) + \mathcal{E}_{int}(\phi) \quad (1)$$

where $\mathcal{E}_{ext}(\phi)$ is external energy that depends upon the data of interest (see below), and $\mathcal{E}_{int}(\phi)$ is the internal energy that penalizes the deviation of the level set function from a signed distance function [12]. In image segmentation, active contours are dynamic curves that move toward the object boundaries. To achieve this goal, we explicitly define an external energy that can move the zero level curves toward the object boundaries. The external energy is defined by

$$\mathcal{E}_{ext}(\phi) = \lambda \mathcal{A}_g(\phi) + v \mathcal{L}_g(\phi) \quad (2)$$

where $\lambda \in \Re$ and $v > 0$ are the constant parameters that weight the energy terms $\mathcal{A}_g(\phi)$ and $\mathcal{L}_g(\phi)$, which are defined by

$$\mathcal{A}_g(\phi) = \int_{\Omega} g H(-\phi) dx dy, \quad (3)$$

and

$$\mathcal{L}_g(\phi) = \int_{\Omega} g \delta(\phi) |\nabla \phi| dx dy \quad (4)$$

where H is the Heaviside function, and δ is the univariate Dirac function. The energy $\mathcal{A}_g(\phi)$ is introduced to speed up the motion of the zero level contours in the level set evolution process, when the edge indicator function g is constant 1, consequently, the energy $\mathcal{A}_g(\phi)$ is exactly the area of the region $\Omega_{\phi}^- = \{(x, y) | \phi(x, y) < 0\}$. Hence, this energy is necessary when the initial contour is placed far away from the desired object boundaries. The energy $\mathcal{L}_g(\phi)$ computes the length of the edge indicator function g along the zero level curves in the conformal metric $ds = g(\mathcal{C}(q)) |\mathcal{C}'(q)| dq$, furthermore, it is minimized when the zero level curve of ϕ is located at the object boundaries. An internal energy $\mathcal{E}_{int}(\phi)$ will be defined in Section III in an application of the general formulation (1) to image segmentation. The minimization of the energy $\mathcal{E}(\phi)$ can be achieved by solving a level set evolution equation, which will be also given in Section III.

In [5], the choice of the edge indicator function [5] is $g = 1/(1 + |\nabla u|)$, which is designed such that it achieves a minimum when the zero level set is located at highest gradient. In our algorithm, we want g to have the smallest value at the

location where the likelihood of having the boundary is minimum. In this paper, we assume that all input segmented images are independently created. We denote P_{dk} and P_{fk} as the probabilities that a boundary pixel of the k^{th} input segmented image is correctly and incorrectly identified, respectively. Next, we need to extract boundaries in the input segmented images. Here, we let u_k be the k^{th} input segmented image. The boundary can be extracted using

$$x_k = \frac{1}{1 + |\nabla G_{\sigma} * u_k|^2} \quad (5)$$

where $G_{\sigma} * u_k$, a smoother part of the image k , is the convolution of the image u_k and Gaussian kernel: $\nabla G_{\sigma}(x, y) = \sigma^{-1/2} e^{-|x^2+y^2|/4\sigma}$, with standard deviation σ . The output image x_k is zero at the outstanding boundaries, and one inside the segmented regions. However, there are the transition regions between segments where the value of x_k changes from one to zero and one. After that, we use the Chair-Varshney fusion rule for calculating a novel edge indicator function g that can be written in follow general summation form:

$$g = - \sum_{k=1}^K \left[(1 - x_k) \log \frac{P_{dk}}{P_{fk}} + x_k \log \frac{1 - P_{dk}}{1 - P_{fk}} \right] \quad (6)$$

where K is a number of input segmented images. This optimal fusion rule is essentially a weighted sum of image, and it requires the knowledge of segmentation accuracies. To examine edge indicator function, if any image density of x_k is zero that implicitly is outstanding edge, the weight of its point will be $\log \frac{P_{dk}}{P_{fk}}$ which is a log-likelihood ratio that a pixel is at the boundary when the k^{th} segmented image indicates that it is. On the other hand, if image density of x_k is one that is inside segmented region, the weight of its point will be $\log \frac{1 - P_{dk}}{1 - P_{fk}}$ which is a log-likelihood ratio that a pixel is at the boundary when the k^{th} segmented image indicates that it is not.

We use an image of a white rectangular object, as shown in Fig. 1(a), to make decision of the edge indicator function in Eq. (6). Fig. 1(b) shows the smooth edge detection of this object. It means that the outstanding edge is zero, and the inhomogeneous region is one. The edge indicator function of this rectangular object based on Chair-Varshney rule is shown as Fig. 1(c), with $P_d = 0.99$ and $P_f = 0.05$.

In level set theory, we cannot directly sum the weight of each k^{th} image together. Not only is these weights varying around zero as shown in Fig. 1(c), but these also are not zero except unexpected case $P_{dk} = P_{fk}$. We are interested in this problem because the minimization of energy terms $\mathcal{A}_g(\phi)$ and $\mathcal{L}_g(\phi)$, which the edge indicator function is assembled, have to be zero. Therefore, we propose supplementary process for dealing with the mentioned problem. In practice, our technique is that creating a searching window in order to find a minimum value within window, taking the minimum value to central of

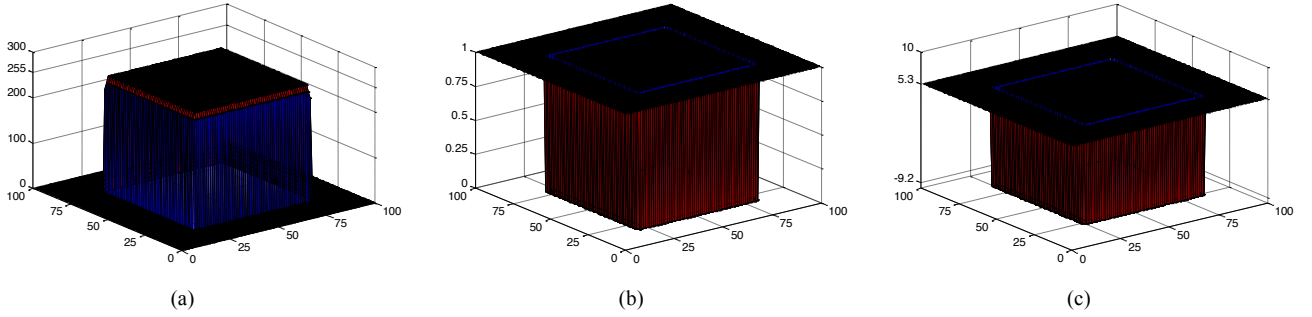


Fig. 1. Surface evolution of a white rectangular object based on the proposed algorithm. (a) shows the value of each pixel of the white rectangular object, (b) shows the smooth edge detection, and (c) shows the edge indicator function of the with probability of image performance $P_d = 0.99$ and $P_f = 0.05$, respectively.

window, and moving the window throughout the image. Size of window is $n \times n$, when n have to be odd number. Next, we totally sum all results of each image together. To keep with the constraint of level set method, we must subtract the image by its minimum value in order to make negative weighting value to be zero.

III. APPLICATION TO EDGE-BASED ACM

The proposed edge indicator function in (6) can be applied to the level set formulation for embedding the zero level set as provided object boundary. In this section, we offer not only an application of the edge indication function to an edge-based active contour model, but also the straightforward implementation of our algorithm.

A. Level Set Method for Image Segmentation

For a level set function $\phi : \Omega \rightarrow \mathbb{R}$, we define an energy functional $\mathcal{E}(\phi)$ by

$$\mathcal{E}(\phi) = \lambda \mathcal{A}_g(\phi) + \nu \mathcal{L}_g(\phi) + \mu \mathcal{R}_p(\phi) \quad (7)$$

where $\mu > 0$ is a constant parameter, and $\mathcal{R}_p(\phi)$ is the level set regularization term [8], which is expressed by

$$\mathcal{R}_p(\phi) = \int_{\Omega} p(|\nabla \phi|) dx dy \quad (8)$$

where p is a potential (or energy density) function $p : [0, \infty) \rightarrow \mathbb{R}$. This regularization term $\mathcal{R}_p(\phi)$ forces $|\nabla \phi|$ to be zero that is minimization when $|\nabla \phi| = 1$. The corresponding level set regularization term $\mathcal{R}_p(\phi)$ is referred to as a distance regularization term for its role of maintaining the signed distance property of the entire domain. A definition of the potential [9] for distance regularization is

$$p(z) = \begin{cases} \frac{1}{(2\pi)^2} (1 - \cos(2\pi z)), & \text{if } z \leq 1 \\ \frac{1}{2}(z - 1)^2, & \text{if } z > 1. \end{cases} \quad (9)$$

This equation shows that the energy density $p(z)$ has two minimum points at $z=0$ and $z = 1$. Using this potential not

only avoids the side effect that occurs in [8], but also offers some appealing theoretical and numerical properties of the level set evolution. Now, the total energy functional $\mathcal{E}(\phi)$ in (7) can be approximated by

$$\begin{aligned} \mathcal{E}(\phi) = & \lambda \int_{\Omega} g H(-\phi) dx dy + \nu \int_{\Omega} g \delta(\phi) |\nabla \phi| dx dy \\ & + \mu \int_{\Omega} p(|\nabla \phi|) dx dy. \end{aligned} \quad (10)$$

By calculus of variations [10], the steepest descent process for minimization of the total energy functional in eq. (10) can be performed by solving the following gradient flow equation:

$$\begin{aligned} \frac{\partial \phi}{\partial t} = & \lambda g \delta(\phi) + \nu \delta(\phi) \operatorname{div} \left(g \frac{\nabla \phi}{|\nabla \phi|} \right) \\ & + \mu \operatorname{div} (d_p(|\nabla \phi|) \nabla \phi) \end{aligned} \quad (11)$$

where d_p is a function defined by $d_p(z) = p'(z)/z$, and $\operatorname{div}(\cdot)$ is the divergence operator. Note that eq. (11) is an edge-based geometric active contour model, which is an application of the edge indicator function (6). This gradient flow, which is an edge-based geometric active contour model, is the evolution equation of the level set function. The first and second terms on the right hand side in eq. (11) are associated with the energy terms $\mathcal{A}_g(\phi)$ and $\mathcal{L}_g(\phi)$ respectively, while the third term is associated with the distance regularization energy $\mathcal{R}_p(\phi)$. In this paper, we use level set method that take negative values inside the zero level contour and positive values outside. In this case, if the initial contour is located inside the object, the parameter λ in the weighted energy $\mathcal{A}_g(\phi)$ should take negative value to expand the contour. If the initial contour is located inside the object, the parameter λ should be positive, so that the zero level contours can shrink in the level set evolution.

B. Numerical Implementation

The implementation of our method is straightforward. The Dirac delta function in (11) can be approximated by the following smooth function $\delta_\epsilon(x)$, defined by

$$\delta_\varepsilon(x) = \begin{cases} \frac{1}{2\varepsilon} \left[1 + \cos\left(\frac{\pi x}{\varepsilon}\right) \right], & |x| \leq \varepsilon \\ 0, & |x| > \varepsilon \end{cases} \quad (12)$$

Generally, the parameter ε is set to 2.0 for our experiments. While the initial level set function ϕ_0 is defined as a following binary step function:

$$\phi_0(\mathbf{x}) = \begin{cases} -\kappa, & \text{if } \mathbf{x} \in R_0 \\ \kappa, & \text{otherwise} \end{cases} \quad (13)$$

where κ is a positive constant, and R_0 is an arbitrary region in the image domain Ω . The initial function ϕ_0 will evolve stably according to the temporal partial derivative $\partial\phi/\partial t$, which can be discretized as $(\phi_{i,j}^{k+1} - \phi_{i,j}^k)/\Delta t = H(\phi_{i,j}^k)$, where $\phi_{i,j}^k$ is a discretized form of level set function $\phi(t, x, y)$ with spatial index (i, j) as well as temporal index k , and $H(\phi_{i,j}^k)$ is the approximation of the right hand side in (10). Therefore, this difference equation can be express as

$$\phi_{i,j}^{k+1} = \phi_{i,j}^k + \Delta t H(\phi_{i,j}^k) \quad (14)$$

which is an iteration process used in the numerical method of our experiment. Note that selection of time step Δt must satisfy $\Delta t < 1/4\mu$ in order to maintain stable level set evolution. Using larger time step can speed up the evolution, but may cause error in the boundary location if the time step is chosen too large. There is a tradeoff between choosing larger time step and accuracy in boundary location.

IV. EXPERIMENTAL RESULTS

This section presents the numerical results of proposed algorithm for the synthetic images, with different knowledge of image performance. In our experiments, we show the result of the active contour evolving in a 100×100 -pixel image, which is fused from two different source images. However, adjusting various level set parameters individually rely on the suitability of each experiment. Moreover, we separate each experiment into three sub-experiments. As the appropriateness of meeting the accurate final fused edge boundaries, probability of false alarm is assumed to be small value 0.5% in all sub-experimental. Furthermore, we assume the P_d of first image more than the second image, conversely fix P_d of first image less than the second image, and finally fix P_d of first image as much as the second image in first, second and third sub-experiment, respectively. In addition, we clearly list the probability parameters of each sub-experiment as shown in Table 1.

In first experiment, Fig. 2 shows the results of final decision boundaries on a fused image from two source images, which are generated from one large quadrilateral object and four small quadrilateral objects. In this case, the initial level set ϕ_0 was firstly calculated from the region enclosed by the rectangular enclosing. The evolution of level set function ϕ in each sub-experiment is also presented in each row of Fig. 2. by contouring the zero level curves with the red thicker ones. For these images, we used the level set parameters $\lambda = 1.0$, $\nu = 4.5$,

$\mu = 4.0$, $\Delta t = 0.05$, and 9×9 searching window. The curve evolution takes 800, 600, and 650, respectively.

In our second experiment, Fig. 3 presents two original images that are an oblique and a non-oblique rectangular object, and advanced results of final decision edge on the fused image. In this case, the initial level set ϕ_0 was also computed from the region enclosed by the rectangular enclosing as previous experiment. However, the evolution of level set function ϕ in all three sub-experiments is showed in second row of Fig. 3. For these resulting images, we used the level set parameters $\lambda = 1.0$, $\nu = 6.5$, $\mu = 4.0$, $\Delta t = 0.05$, and 11×11 searching window. The curve evolution takes 700, 600, and 900, respectively.

For our several results, it can be clearly seen that stopping of active contour depends on not only the zero level curve, but also probabilities of image performance. Whenever false alarm probability of each source image is smallest value, the zero level curve will consequently stop at the boundaries of image that has higher detection probability.

TABLE I
PROBABILITY PARAMETERS OF EXPERIMENTS

Probability parameters	1 st image		2 nd image	
	P_d	P_f	P_d	P_f
1 st sub-experiment	0.99	0.005	0.5	0.005
2 nd sub-experiment	0.5	0.005	0.99	0.005
3 rd sub-experiment	0.5	0.005	0.5	0.005

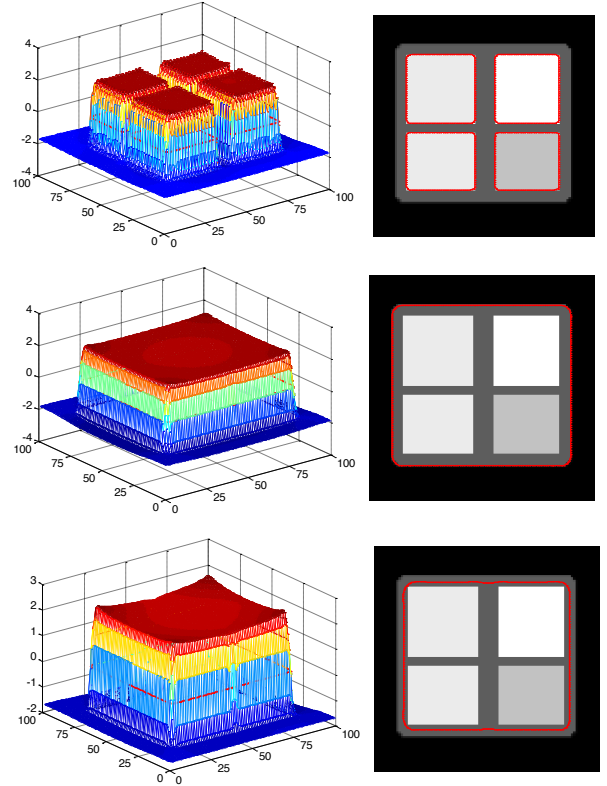


Fig. 2. Evolution of level set function and its results for the fused image from two source synthetic images in respective sub-experiment, with $\lambda = 1.0$, $\nu = 4.5$, $\mu = 4.0$, $\Delta t = 0.05$, and 9×9 searching window.

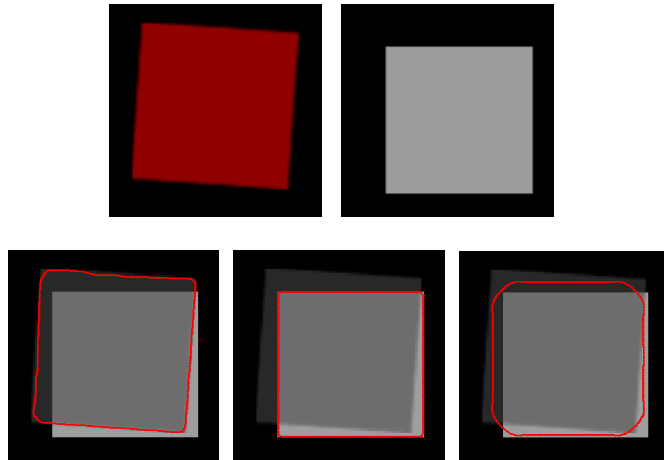


Fig. 3. Upper row: two original images. Lower row: advanced results for the edge fusion image in respective sub-experiment, with $\lambda = 1.0$, $\nu = 6.5$, $\mu = 4.0$, $\Delta t = 0.05$, and 11×11 searching window.

V. CONCLUSION

In this paper, we presented an automatic segmentation approach based on level set formulation and a new technique for deciding final edge fusion. Furthermore, our segmentation model used an edge-based active contour model and the Chair-Varshney fusion rule, which bases on a log likelihood ratio test, in order to serve the purpose of stopping the evolving curve on the final decision boundaries by applying general edge indicator function to the novel effective model. Our preliminary results show the progress that is able to be performed the classification or segmentation label relying on probabilities of image performance as well as conditional observation process.

REFERENCES

- [1] S. Osher and J. Sethian, "Fronts propagating with curvature-dependent speed: Algorithms based on Hamilton-Jacobi formulations," *J. Comput. Phys.*, vol. 79, no. 1, pp. 12–49, Nov. 1988.
- [2] V. Caselles, F. Catte, T. Coll, and F. Dibos, "A geometric model for active contours in image processing," *Numer. Math.*, vol. 66, no. 1, pp. 1–31, Dec. 1993.
- [3] R. Malladi, J. A. Sethian, and B. C. Vemuri, "Shape modeling with front propagation: A level set approach," *IEEE Trans. Pattern. Anal. Mach. Intell.*, vol. 17, no. 2, pp. 158–175, Feb. 1995.
- [4] M. Kass, A. Witkin, and D. Terzopoulos, "Snakes: Active contour models," *Int. J. Comput. Vis.*, vol. 1, no. 4, pp. 321–331, Jan. 1987.
- [5] V. Caselles, R. Kimmel, and G. Sapiro, "Geodesic active contours," *Int. J. Comput. Vis.*, vol. 22, no. 1, pp. 61–79, Feb. 1997.
- [6] C. Gout, C. Le Guyader, and L. Vese, "Segmentation under geometrical conditions with geodesic active contour and interpolation using level set methods," *Numerical Algorithms*, Vol.39, pp. 155–173, 2005.
- [7] T. Chan and L. Vese, "Active contours without edges," *IEEE Trans. Imag. Proc.*, vol. 10, pp. 266–277, 2001.
- [8] C. Li, C. Xu, C. Gui, and M. D. Fox, "Level set evolution without re-initialization: A new variational formulation," *inProc. IEEE Conf. Comput. Vis. Pattern Recognit.*, vol. 1, pp. 430–436, 2005.
- [9] C. Li, C. Xu, C. Gui, and M. D. Fox, "Distance regularized level set evolution and its application to image segmentation," *IEEE Trans. Image Process.*, vol. 19, no. 12, pp. 3243–3254, Dec. 2010.
- [10] B. A. Dubrovin, A. T. Fomenko, and S. P. Novikov, *Modern Geometry - Methods and Applications, Part I: The Geometry of Surfaces, Transformation Groups, and Fields*. Springer-Verlag, New York, 1984.
- [11] Z. Chair and P.K.Varshney, "Optimal data fusing in multiple sensor detection system," *IEEE Trans. Aerospace Election Syst.* pp.98-101.Jan.22 1986.
- [12] M. Sussman, P. Smereka, and S. Osher, "A level set approach for computing solutions to incompressible two-phase flow," *J. Comput. Phys.*, vol. 114, no. 1, pp. 146–159, Sep. 1994.
- [13] R. Ronfard, "Region-based strategies for active contour models," *Int. J. Comput. Vis.*, vol. 13, no. 2, pp. 229–251, Oct. 1994.
- [14] D. Lu and Q. Weng, "A survey of image classification methods and techniques for improving classification performance," *Inter. J. Remote Sens.*, vol. 28, no. 5, pp. 823–870, March 2007
- [15] S. Osher and R. P. Fedkiw, *Level set methods and dynamic implicit surfaces*. Springer, NY: Applied Mathematical Science, 2003.